Since January 2020 Elsevier has created a COVID-19 resource centre with free information in English and Mandarin on the novel coronavirus COVID-19. The COVID-19 resource centre is hosted on Elsevier Connect, the company's public news and information website.

Construction and Building Materials 344 (2022) 128245

Contents lists available at ScienceDirect

Construction and Building Materials

journal homepage: www.elsevier.com/locate/conbuildmat

Effective recycling of disposable medical face masks for sustainable green concrete via a new fiber hybridization technique

Wisal Ahmed [a], C.W. Lim [a,b,*]

[a] Department of Architecture and Civil Engineering, City University of Hong Kong, Kowloon, Hong Kong Special Administrative Region
[b] City University of Hong Kong Shenzhen Research Institute, Shenzhen 518057, PR China

ARTICLE INFO

Keywords:
Basalt fiber
DMFM fiber
Flexural strength
Mechanical properties
Splitting tensile strength
Sustainable concrete

ABSTRACT

Global public response to the COVID-19 (SARS-CoV-2) pandemic is highly focused on human health. However, conservationists have cautioned of unprecedented threats to the natural environment from a new type of non-biodegradable microplastic waste resulting from extensive use of disposable medical face masks (DMFMs). Thus, this waste must be recycled in an eco-friendly manner on an urgent basis. In this research, we developed a new environmentally friendly recycling technique using waste DMFMs in sustainable green concrete. More explicitly, a new fiber hybridization approach has been introduced in which two types of fibers namely DMFM fiber and basalt fiber (BF) were incorporated into fiber reinforced recycled aggregate concrete (FRAC). The volume fractions of DMFM fiber were 0%, 0.1%, and 0.2% and the volume fractions of BF were 0%, 0.25%, and 0.5%. In addition, two mineral admixtures (fly ash and ground granulated blast furnace slag) were also used. Test results indicated increase of approximately 12% in compressive strength, 26% in split tensile strength, and 60% in flexural strength of FRAC containing hybrid fibers and mineral admixtures. The density and ultra-sonic pulse velocity (UPV) of DMFM fiber- and BF-modified FRAC ranged from 2406–2433 kg/m^3 and 4502–4541 m/s, respectively, which meets structural concrete requirements. The water absorption rate gradually increased with an increase in the volume fractions of fibers but remained within the allowable water absorption limit for construction materials. Lastly, the microstructure investigation indicated excellent concrete quality, improved interfacial transition zones (ITZs), and good compatibility of host concrete matrix with both DMFM fiber and BF that correlates well with the experimental results reported in this study.

1. Introduction

The ongoing COVID-19 (SARS-CoV-2) pandemic that began in late 2019 has affected the entire world, resulting in massive human loss, devastating social and economic disruptions, and unprecedented challenges to the global environment. Despite the rapid global vaccination drive, several variants of SARS-CoV-2 including Alpha (B.1.1.7), Beta (B.1.351), Gamma (P.1), Delta (B.1.617.2), and Omicron (B.1.1.529) have emerged so far that resulted in more than 5.5 million fatalities worldwide [1,2]. The global public response is intensively focused on protection of human life; however, conservationists have cautioned of severe repercussions to the natural environment from a rapidly growing volume of non-biodegradable plastic waste extending well beyond the pandemic [3,4].

To contain the spread of the novel coronavirus and mitigate the emergence of subsequent COVID-19 waves, personal protective equipment (PPE) such as face masks was recommended by the World Health Organization (WHO) in its interim guidance issued on January 29, 2020 [5,6]. Since then, many nations and regions have initiated special COVID-19 prevention measures including mandatory face masks in public settings. Consequently, global use of face masks, especially disposable medical face masks (DMFMs), has soared to unprecedented levels. Before COVID-19, the annual global market for face masks was estimated to be approximately $0.73 billion; it is now expected to exceed $22 billion [7]. Due to a lack of environmental protection measures and public negligence, DMFMs are being discarded openly in the environment, in public places such as parks, streets, highways, beaches, and sewage channels resulting in tens of thousands of tons of non-biodegradable micro-plastic waste that eventually pollutes the natural environment [8,9]. The findings of recent surveys conducted in Bangkok [7], Lima city [8], Chile [10], Australia [11], South America [12], Europe [13], Africa [14], and the Arabian Peninsula [15] indicate a massive increase in waste PPEs since the start of the COVID-19

* Corresponding author at: Department of Architecture and Civil Engineering, City University of Hong Kong, Kowloon, Hong Kong Special Administrative Region.
E-mail address: bccwlim@cityu.edu.hk (C.W. Lim).

https://doi.org/10.1016/j.conbuildmat.2022.128245
Received 18 April 2022; Received in revised form 5 June 2022; Accepted 21 June 2022
Available online 27 June 2022

Nomenclature

Acronyms

BF	basalt fiber
C-A-S-H	calcium alumino-silicate hydrate
C-S-H	calcium silicate hydrate
DMFMs	disposable medical face masks
EDAX	energy dispersive spectroscopy
FA	fly ash
FRAC	fiber reinforced recycled aggregate concrete
GGBFS	ground granulated blast furnace slag
ITZs	interfacial transition zones
MPa	megapascal
NAC	normal aggregate concrete
NCA	normal concrete aggregate
NFA	natural fine aggregate
OPC	ordinary Portland cement
PCE	polycarboxylic-ether
PP	polypropylene
PPE	personal protective equipment
RAC	recycled aggregate concrete
RCA	recycled concrete aggregate
SEM	scanning electron microscopy
UPV	ultra-sonic pulse velocity
WHO	world health organization
f'_{CS}	compressive strength
f'_{FS}	flexural strength
f'_{ST}	splitting tensile strength
β_{CS}	enhancement coefficient for compressive strength
β_{ST}	enhancement coefficient for splitting tensile strength
β_{FS}	enhancement coefficient for flexural strength

pandemic. Other studies have reported the densities of waste PPE items to be approximately 0.005–0.3 items per square meter of area, which is a significantly high value [9,16]. The repercussions of this have led to a massive increase in global plastic waste and serious threats to the natural environment as the thermoplastic polymer in DMFMs requires up to several decades for its complete natural decomposition [17–19].

Disposal of waste face masks without endangering public health or the natural environment is a major challenge in the post COVID-19 era. The current practices for disposing of these wastes include landfilling and incineration, which may not be the most effective solutions in terms of environmental and public health safety concerns [20,21]. In contrast, the use of waste DMFMs as reinforcing fiber in construction materials is an effective and eco-friendly approach to resolving the global challenge of waste face mask disposal [22,23]. Face masks are commonly made of polypropylene (PP) fiber material that can be used as reinforcement material in concrete [24]. Alabduljabbar et al. [25] used waste PP carpet fiber in conjunction with palm oil fuel ash and reported improvements of approximately 26% and 20% in splitting tensile strength and flexural strength of concrete, respectively. Alrshoudi et al. [26] reported that waste PP fiber can effectively improve concrete impact resistance and ductility due to its crack-bridging and reinforcing abilities. It enhances concrete resistance against creep and early shrinkage, and reduces chloride penetration and carbonation depth, resulting in a durable concrete matrix [27,28]. However, it has been reported that waste PP fiber adversely affects concrete workability and compressive strength. Thus, researchers recommend the use of mineral admixtures with PP fiber in concrete [26,29].

Use of recycled PP fibers extracted from face masks in concrete is a new research area. To date, few research studies in the literature have assessed the basic mechanical properties of normal aggregate concrete containing only face mask fiber [30,31]. This study is a step forward in this regard, with a new fiber hybridization approach to produce a synergistic effect between DMFM fiber and basalt fiber (BF), and improve the physical properties and mechanical performance of fiber reinforced recycled aggregate concrete (FRAC). Two mineral admixtures, fly ash (FA) and ground granulated blast furnace slag (GGBFS), were also used together with the two fibers. To assess the performance of this new eco-friendly and sustainable concrete product, a series of laboratory experiments were conducted including flexural strength, splitting tensile strength, compressive strength, ultrasonic pulse velocity, density, and water absorption tests. In addition, the microstructure of FRAC was inspected to assess the concrete quality and compatibility of DMFM fiber and BF with the concrete matrix. The synergy of DMFM fiber and BF in FRAC was studied via the enhancement coefficients β_{CS}, β_{ST}, and β_{FS} which help assess the performance of the two fibers in single and hybridization modes. Recycling DMFMs as reinforcing fiber for production of green sustainable FRAC would help resolve the rapidly growing plastic waste problem, reduce the burden on landfill sites, and protect the environment.

2. Current statistics and environmental impacts of DMFMs

To determine current DMFM waste statistics and the associated environmental challenges, we must estimate the number of daily discarded waste face masks for world regions including Asia, Africa, Europe, Latin America, the Caribbean, North America, Oceania, and subregions in Asia. Based on the latest population statistics reported by Worldometer [32], and the literature [3,33], the total daily number of discarded facemasks was calculated using the following equation.

$$\text{Total daily discarded DMFMs} = 1 \times 10^{-4} \times (P_{Total} \times P_{Urban} \times A \times B).$$

where P_{Total}, P_{Urban}, A, and B, represent the total population of each region/subregion, the urban population of each region/subregion, the facemask wearing acceptance rate, and daily per person usage of facemasks, respectively.

Data for P_{Total} and P_{Urban} were obtained from Worldometer [32], the facemask wearing acceptance rate (A) and daily per person usage of facemasks (B) were chosen as 80% and 1, respectively [3,33]. According to the statistics shown in Fig. 1, the current daily estimated number of DMFMs is approximately 3503.7 million worldwide. Asia is currently the largest source of global waste DMFMs (1889.8 million daily), followed by Africa (469.7 million), Europe (445.6 million), Latin America and the Caribbean (431.6 million), North America (243.7 million), and Oceania (23.1 million). From Fig. 2, China is the largest contributor in Asia, with a total daily waste DMFM production of approximately 704.0 million, approximately 37.2% of the total DMFM waste in Asia, followed by India (386.4 million), Indonesia (123.4 million), Japan (92.9 million), Pakistan (62.0 million), and Bangladesh (51.9 million). The daily DMFM waste of other Asian countries is presented in Fig. 2.

The estimated DMFM plastic waste in tons produced in different world regions and Asian countries is shown in Figs. 3 and 4, respectively. Assuming a single DMFM weight of 4 g, the estimated daily DMFM waste represents approximately 14,015 tons of plastic waste worldwide. From Fig. 3, approximately 7559 tons of DMFM plastic waste are generated in Asia alone. Africa, Europe, Latin America and the Caribbean, North America, and Oceania produce approximately 1879 tons, 1782 tons, 1726 tons, 975 tons, and 93 tons of DMFM plastic waste, respectively. As expected, China produces the largest quantity of DMFM plastic waste in Asia, an estimated 2816 tons daily. This will further exacerbate the ongoing plastic waste-related issues as the commonly used DMFMs are made up of non-biodegradable plastic material that may require several

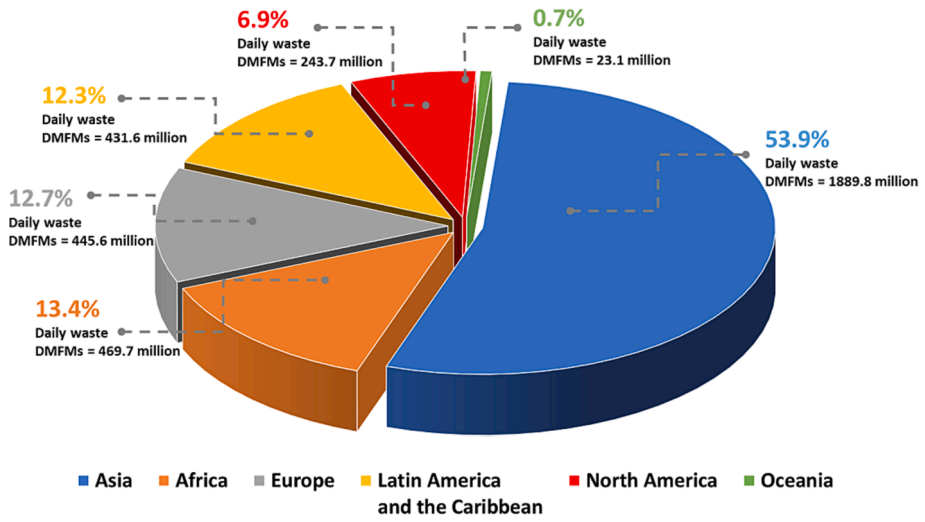

Fig. 1. Current estimated daily DMFM waste in different regions of the world, based on latest Worldometer data [32].

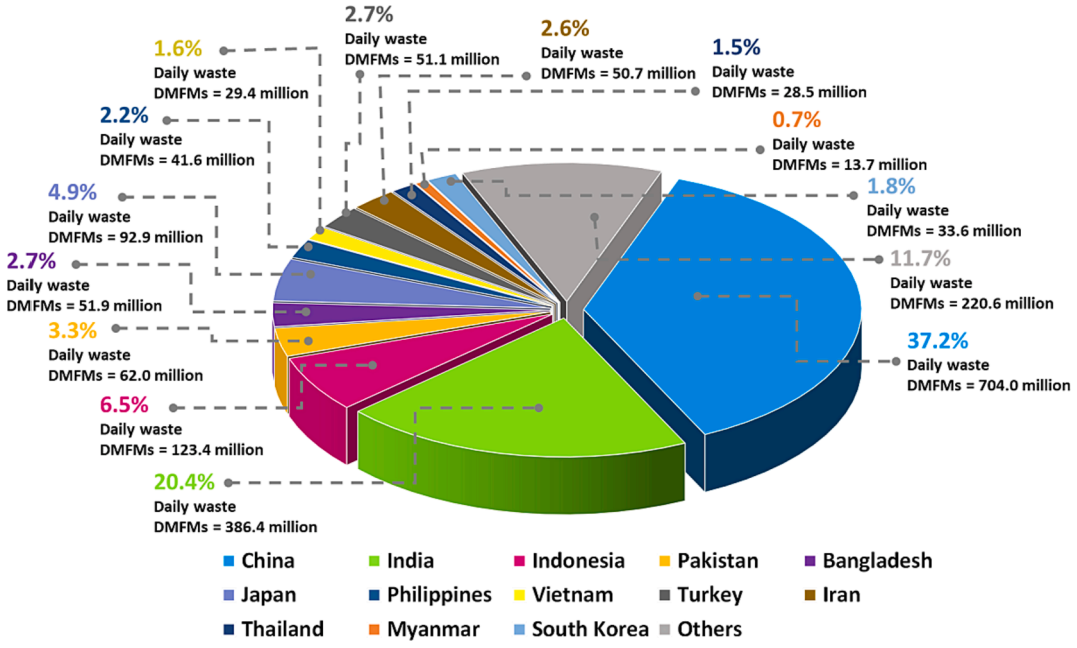

Fig. 2. Current daily DMFM waste statistics for countries in Asia, based on latest Worldometer data [32].

decades for complete decomposition [17,34]. Furthermore, improper disposal of face masks poses a high risk to the health of solid waste collectors and the public as they may contain traces of SARS-CoV-2. Improper disposal of waste DMFMs may affect tourism and result in soil and water contamination [35]. There is now evidence that most of the waste PPE ends up in the ocean due to improper disposal in coastal areas and through surface runoff, presenting an unprecedented risk to marine wildlife and ecosystems [16]. DMFMs usually contain chemical compounds such as surfactants and dyes; their leachability and solubility in the ocean can contaminate the food for aquatic organisms. According to a recently published report by OceansAsia [19], approximately 100,000 marine creatures are affected annually by plastic waste pollution, leading to a $13 billion loss to the global economy. If not resolved, these challenges to public health and the environment will cost the world for decades to come. Thus, waste DMFMs must be recycled in an effective and environmentally friendly manner.

3. Materials and methods

3.1. Materials

3.1.1. Fiber material

To comply with current COVID-19 preventive measures set forth by the Hong Kong government and to prevent adverse response from the community, we used new and unused 3-ply DMFMs in this study that were acquired from a manufacturer in China. The length and width of the DMFMs were about 175 mm and 95 mm, respectively. The top and bottom layers of the DMFMs were made of non-woven PP fiber material and the middle filtering layer was made of melt-blown fabric [36]. The metal nose wire frame and two ear-straps were removed to ensure homogeneity of the fiber material. The DMFMs were reduced to suitable geometric configurations for use in FRAC. The length and width of the DMFM fiber were approximately 20 mm and 5 mm, respectively. The DMFM fiber was used in suitable proportions in FRAC in single and hybrid modes with BF. BF was chosen for its high strength, small

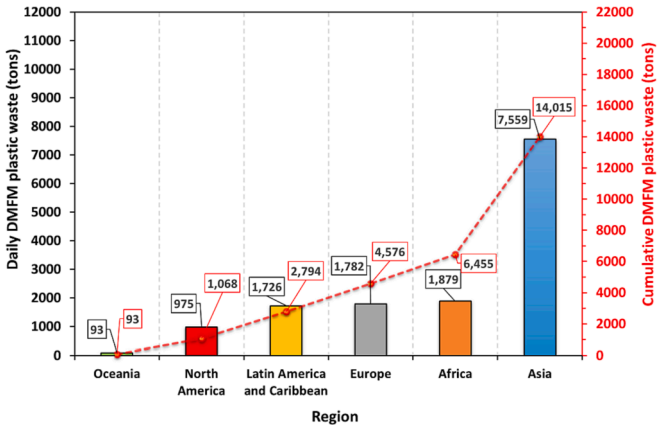

Fig. 3. Estimated daily DMFM plastic waste in different regions in the world. The bar chart shows the daily DMFM plastic waste in tons (left axis); the line graph shows the cumulative plastic waste in tons (right axis).

diameter, and high thermal and chemical stability [22]. In addition, BF is an environmentally friendly and sustainable fiber material requiring less energy resources and no additives during production [37]. The BF was purchased from a manufacturer in China and had a length and diameter of about 18 mm and 17.4 μm, respectively. DMFM fiber and BF samples are is shown in Fig. 5, and their material properties are presented in Table 1.

3.1.2. Concrete constituent materials

Ordinary Portland cement (OPC) Type-I meeting the standards of ASTM C150 [38] was used in the preparation of concrete samples. Two mineral admixtures, FA and GGBFS were used as binders. OPC, FA, and GGBFS were provided by Green Island Cement Ltd., Hong Kong. The total content of FA and GGBFS was 20% of the OPC; their relative ratio was 1:2 [39]. The material properties of OPC, FA, and GGBFS are presented in Table 2. River sand from a local source in Hong Kong was used as the natural fine aggregate (NFA); crushed stone was used as the natural coarse aggregate (NCA). The specific gravity and density of NFA and NCA were 2.70 and 1560 kg/m^3 and 2.68 and 1530 kg/m^3, respectively. Recycled concrete aggregate (RCA) was self-prepared in the laboratory by crushing the waste concrete (M40) with a mechanical jaw crusher. The RCA percentage was maintained at 50% of the NCA in all concrete formulations. The specific gravity and density of the RCA were 2.50 and 1288 kg/m^3, respectively. The particle size gradation curves of the aggregates are shown in Fig. 6, and meet the standards of ASTM C33 [40]. The ratio of water to binder was maintained at 0.42 for all formulations. To compensate for the low workability, a small dosage of superplasticizer (third-generation polycarboxylic-ether (PCE)) meeting the requirements of ASTM C494 [41] was added. Drinking water was used in the production and curing process of concrete samples.

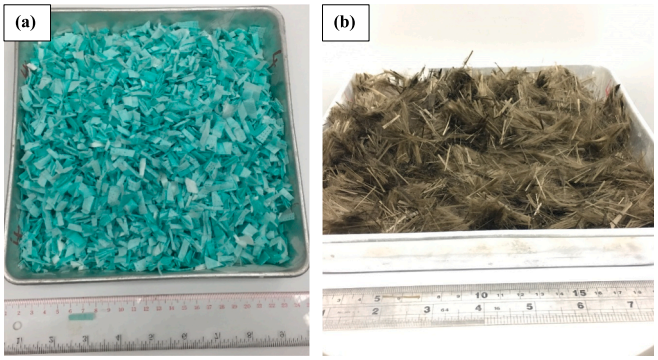

Fig. 5. Samples of fiber materials used in this study; (a) DMFM fiber; (b) BF.

Table 1
Material properties of DMFM fiber and BF.

Fiber	Length (mm)	Width (mm)	Diameter (μm)	Specific gravity	Tensile strength (MPa)	Melting point (°C)
BF	18	–	17.4	2.7	≥2000	1450
DMFM fiber	20	5	–	0.90	≥4.0	160

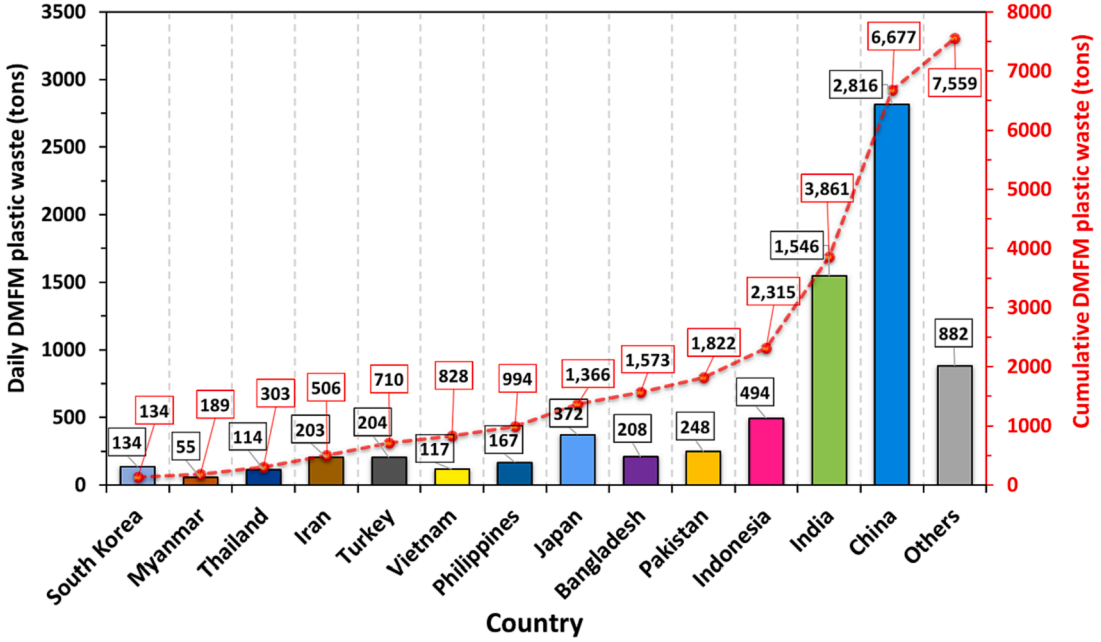

Fig. 4. Estimated daily DMFM plastic waste in Asia. The bar chart shows the daily DMFM plastic waste in tons (left axis); the line graph shows the cumulative plastic waste in tons (right axis).

Table 2
Material properties of OPC, FA, and GGBFS.

Materials	SiO_2 (%)	Al_2O_3 (%)	CaO (%)	Fe_2O_3 (%)	MgO (%)	K_2O (%)	Chloride content (%)	Loss on ignition	Moisture content (%)	Fineness >45 μm (%)
OPC*	20.5	6.6	66.4	3.3	0.7	–	<0.01	3.2	–	–
FA	36.0	25.0	16.5	8.5	1.20	1.20	<0.01	2.9	0.2	8.3
GGBFS	35.3	15.0	38.3	0.9	6.0	0.5	<0.01	0.2	0.2	94.9

*fineness of OPC is 366 m^2/kg.

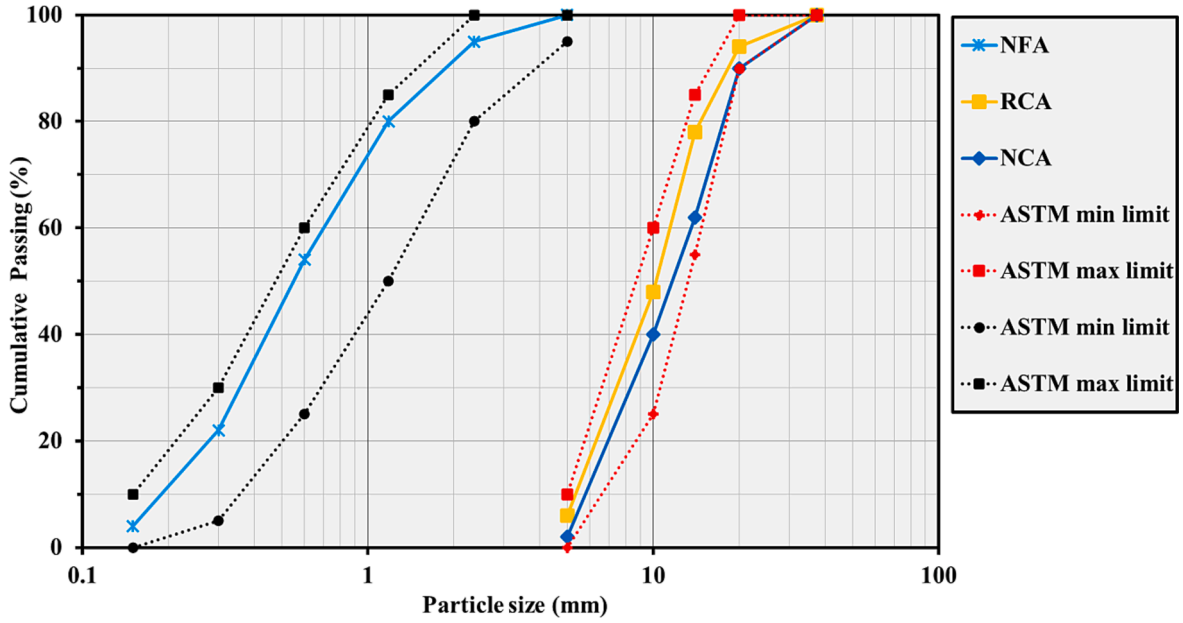

Fig. 6. Particle distribution curves of aggregates. NFA denotes natural fine aggregate, NCA denotes natural coarse aggregate, and RCA denotes recycled concrete aggregate.

3.1.3. Details of concrete mix design

To assess the combined effect of DMFM fiber and BF in fiber-reinforced recycled concrete, ten concrete mix formulations were considered in this research study, as shown in Table 3. The mix formulation designated as M0 was the control formulation, consisting of only concrete constituent materials and no fibers. The M0 mix was used as a reference for modified formulations M1–M9. Mix formulation M1 contained two mineral admixtures (FA and GGBFS) in addition to other concrete constituent materials. Similar to M0, M1 was prepared without fiber materials; its purpose was to investigate the effect of FA and GGBFS on the physical and mechanical properties of recycled concrete. The M2 and M3 mixes contained 0.1% and 0.2% volume fractions of DMFM fiber, respectively. The M4, M5, and M6 mixes comprise 0%, 0.1%, and 0.2% volume fractions of DMFM fiber, respectively, and 0.25% volume fraction of BF. The M7, M8, and M9 mixes contained 0%, 0.1%, and 0.2% volume fractions of DMFM fiber, respectively, and 0.5% volume fractions of BF. The DMFM fiber and BF dosage selection were based on recently reported literature [42,43].

3.2. Sample preparation

A uniform concrete batching and mixing method was used for all concrete mix designs to ensure homogeneity and uniformity of concrete. All concrete constituent materials were added to a power-driven rotating concrete mixer and mixed in a dry state for 30 s. Half of the mix design water was added to the mixture and the mixing process was continued for 1 min. The surface wet aggregate, cement, mineral admixtures (FA and GGBFS), the superplasticizer, and remaining water

Table 3
Details of concrete mix formulations used in this study; 'OPC' represents ordinary Portland cement, 'FA' represents fly ash, 'GGBFS' represents ground granulated blast furnace slag; 'NFA', 'NCA', 'RCA', and 'SP' denote natural fine aggregate, natural coarse aggregate, recycled concrete aggregate, and superplasticizer, respectively.

Mix ID	Fiber dosage (%)		Binder (kg/m^3)			NFA (kg/m^3)	NCA (kg/m^3)	RCA (kg/m^3)	Water (kg/m^3)	SP (%)
	DMFM fiber	Basalt fiber	OPC	FA	GGBFS					
M0	0.00	0.00	489	–	–	867	430	367	205	1.00
M1	0.00	0.00	391	33	65	867	430	367	205	1.00
M2	0.10	0.00	391	33	65	867	430	367	205	1.00
M3	0.20	0.00	391	33	65	867	430	367	205	1.00
M4	0.00	0.25	391	33	65	867	430	367	205	1.00
M5	0.10	0.25	391	33	65	867	430	367	205	1.00
M6	0.20	0.25	391	33	65	867	430	367	205	1.00
M7	0.00	0.50	391	33	65	867	430	367	205	1.00
M8	0.10	0.50	391	33	65	867	430	367	205	1.00
M9	0.20	0.50	391	33	65	867	430	367	205	1.00

were mixed for 3 min. During this time, the fiber materials (DMFM fiber and BF) were gradually added to the mixture to avoid fiber clumping and ensure uniform dispersion of fibers, as suggested in the literature [31,44]. The preparation of FRAC is shown in Fig. 7. The freshly prepared concrete mix was poured into molds and compacted via a vibrating table to remove any entrapped voids. The fresh concrete samples were stored in a laboratory in controlled conditions for 24 h before they were demolded and placed in a water curing tank at 20 ± 2 °C and 95% relative humidity for a curing period of 28 days. The physical and mechanical properties of the concrete samples were tested after the specified curing period.

3.3. Testing procedure

To evaluate the effect of DMFM fiber and BF on the physical and mechanical properties of the FRAC, a series of laboratory experiments were conducted. For splitting tensile and compressive strength tests, concrete cylindrical specimens with height and diameter of 200 mm and 100 mm, respectively, were tested according to standard ASTM C39 [45] and ASTM C496 [46] procedures. The flexural strength test was made via the universal testing machine on concrete prismatic beams with a width and height of 100 mm and length of 400 mm according to the standard ASTM C78 procedure [47]. The concrete uniformity and integrity were assessed via an ultrasonic pulse velocity (UPV) test according to ASTM C597 [48] using 100-mm concrete cubical samples and a PUNDIT ultrasonic pulse/receiver made by C.N.S Electronic Ltd. The concrete density and water absorption were determined according to the standard ASTM 642-06 procedure [49]. In each case, at least three samples were tested; the average value was used for further analysis and discussion. The laboratory test setup is shown in Fig. 8.

4. Results and discussion

4.1. Microstructure and EDAX analysis of fiber

The surface morphologies of DMFM fiber and BF are shown in Fig. 9, captured by a Thermo Fisher Scientific Quattro S Scanning Electron Microscope. The morphology of the outer layer of DMFM fiber visible in Fig. 9(a) reveals a non-woven fabric-type surface morphology made of randomly distributed and closely spaced fibers with an approximate diameter of 36 μm. The fibers are joined together through oval melting junction points spaced several hundred μm apart to form a closely-packed dense microstructure. The surface morphology of the inner layer of DMFM in Fig. 9(b) shows a smooth surface texture of thin PP fiber with an average diameter of approximately 20 μm. It is evident from the micrograph that the inner structure of DMFM contains wide gaps and voids due to the PP fiber arrangement. These DMFM fiber surface morphologies are consistent with observations in previous research [50,51]. In Fig. 9(c), the SEM micrograph of BF reveals a filament-type structure with a uniform circular section. The surface topography of BF shows a relatively smooth surface texture with no visible voids or pores.

Energy dispersive spectroscopy (EDAX) X-ray analysis was performed to characterize the elemental composition of DMFM and BF. The EDAX spectra and percentage distribution of elements present in DMFM fiber and BF samples are shown in Fig. 10. The EDAX spectra of DMFM fiber indicate a sharp high-intensity peak assigned to carbon, representing approximately 98.83% of the atomic weight. Several small peaks are observed that correspond to oxygen (0.91%), silicon (0.15%), and zirconium (0.11%). The EDAX spectra of BF show several sharp peaks that represent various elements. The highest content (atomic%) was oxygen (45.61%), followed by carbon (23.58%), silicon (14.63%), and aluminum (5.59%). Several small peaks were identified that confirm the presence of calcium (2.91%), magnesium (2.71%), sodium (2.29%), iron (2.07%), potassium (0.24%), titanium (0.24%), barium (0.07%), and cobalt (0.05%). Similar SEM-EDAX spectra for DMFM fiber and BF were reported by other researchers [52,53].

4.2. Compressive strength

The compressive strength (*f*'cs) of the reference sample and hybrid fiber-modified recycled concrete samples determined after the 28-day curing period is shown in Fig. 11. It is evident that the *f*'cs of recycled concrete gradually increases with use of fiber materials and mineral admixtures. For M1, M2, and M3 formulations with 0%, 0.1%, and 0.2% DMFM fiber content, respectively, the *f*'cs were 46.9 MPa, 47.1 MPa, and 47.6 MPa, corresponding to increases of about 2.8%, 3.3%, and 4.4%, respectively. The slight increase in the *f*'cs of concrete is mostly

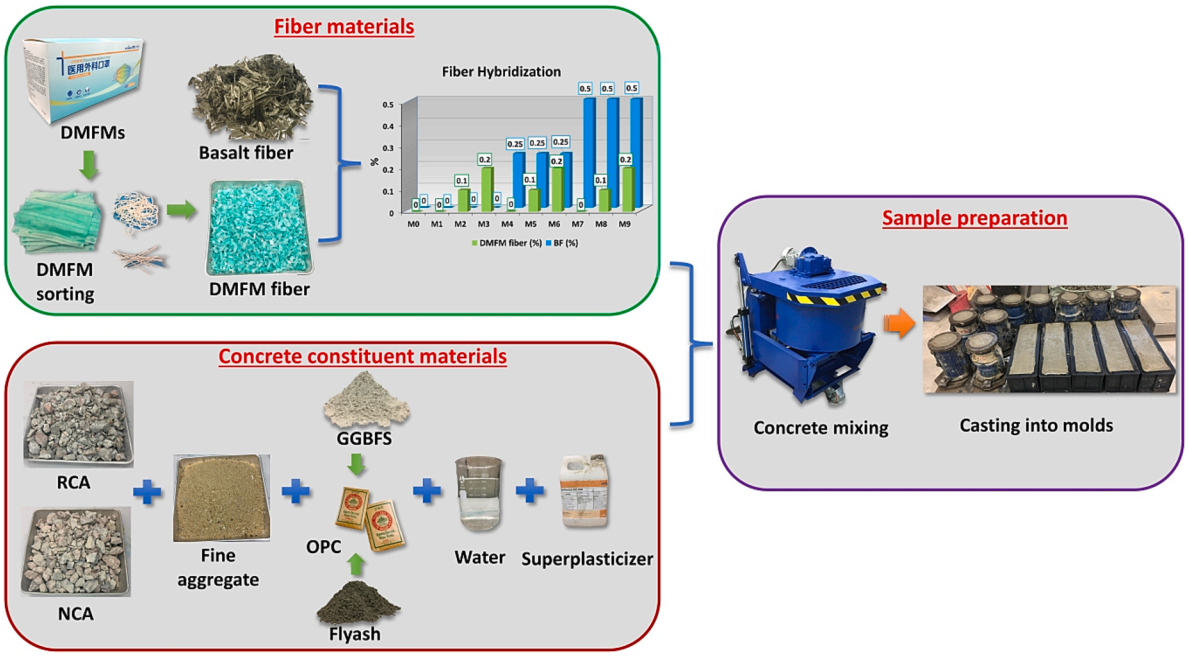

Fig. 7. FRAC production process with DMFM fiber and BF.

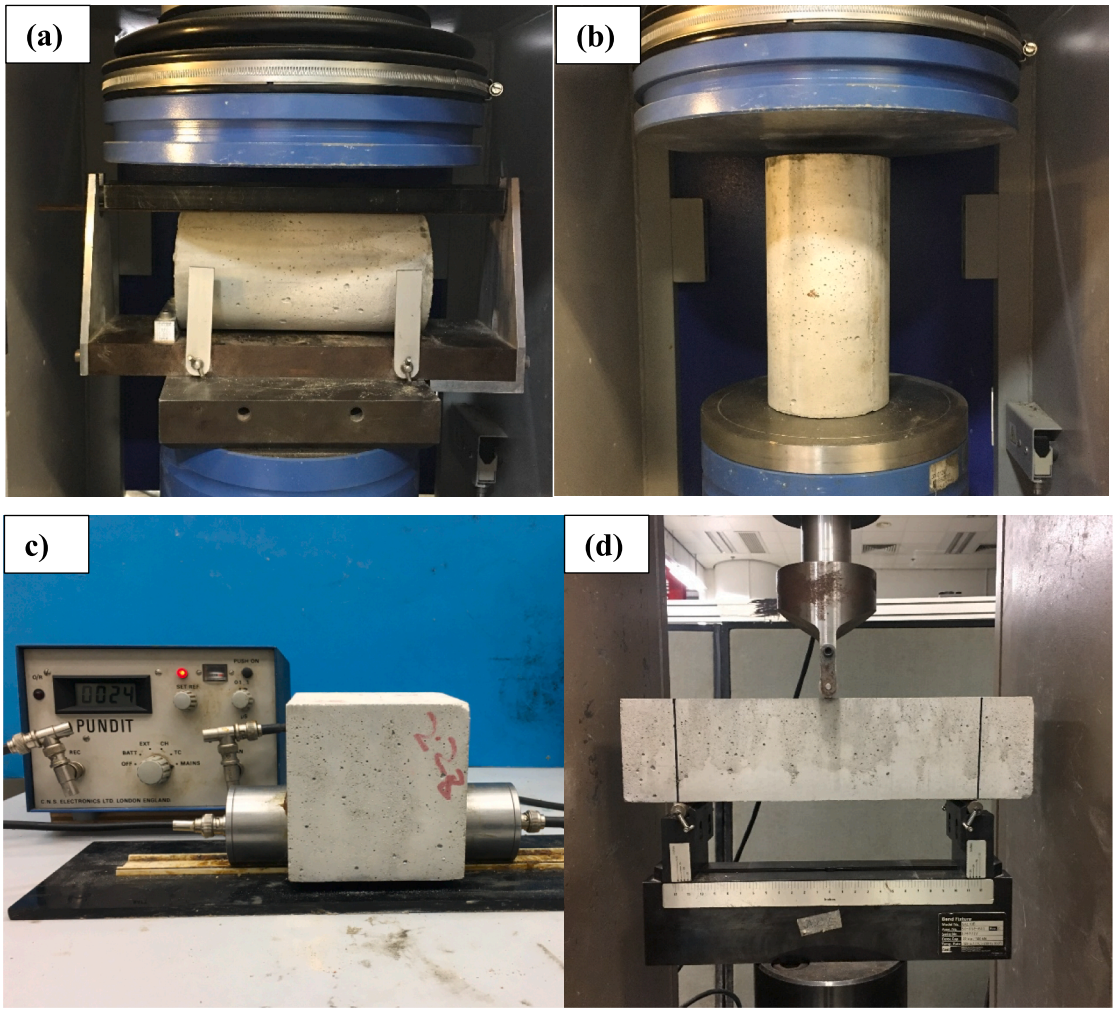

Fig. 8. Test setup for (a) splitting tensile strength test; (b) compressive loading strength test; (c) ultrasonic pulse velocity test; (d) three-point bending test.

due to the addition of FA and GGBFS, as they form additional calcium silicate hydrate (C-S-H) and calcium alumino-silicate hydrate (C-A-S-H) gels, thus improving the concrete strength. Similar observations were made by Banchhor et al. [54] and Rafeet et al. [55]. The $f'cs$ tends to increase further with combined use of DMFM fiber (0–0.2%) and BF (0.25%). The $f'cs$ of M4, M5, and M6 are 47.8 MPa, 48.9 MPa, and 49.9 MPa, representing 4.9%, 7.4%, and 9.4% increases, respectively. Similarly, the $f'cs$ of M7, M8, and M9 indicate further increases with increasing DMFM fiber and BF dosages (0–0.2% and 0.5%, respectively). Of all samples, M8 has the highest $f'cs$ value (51.1 MPa), representing a 12.1% increase compared to the reference sample. The increase in $f'cs$ can be attributed to inclusion of BF, which is known for its crack bridging and reinforcing abilities [22,56]. However, M9 shows a slight reduction in overall $f'cs$ improvement, possibly due to improper concrete mixing resulting from the high fiber dosage [57]. Nevertheless, it is still higher than the reference sample.

The failure mode of the reference sample (M0) and hybrid fiber-reinforced concrete (M8) is shown in Fig. 12. The M0 sample failed abruptly without exhibiting significant cracks, indicating typical concrete compression failure with removal of a large concrete chunk after reaching its ultimate compression strength. In contrast, the surface of the M8 sample exhibited several well-defined cracks distributed along the longitudinal axis of the sample. Unlike the reference sample, M8 retained its structure, with no large concrete chunk removed, possibly attributed to the joint-reinforcing action of DMFM fiber and BF.

4.3. Splitting tensile strength

Fig. 13 shows the splitting tensile strength (f'_{ST}) of the reference sample and hybrid-fiber reinforced recycled concrete samples after the 28-day curing period. The graph indicates significant improvements in the overall tensile capacity of hybrid fiber-reinforced concrete with DMFM fiber and BF. M1, M2, and M3 prepared with only DMFM fiber (0%, 0.1%, and 0.2%) exhibited f'_{ST} of 3.2 MPa, 3.3 MPa, and 3.5 MPa, representing increases of 1.2%, 4.4%, and 9.3%, respectively. The increases in f'_{ST} indicate that the use of DMFM fiber and mineral admixtures collectively improved the cracking resistance of the recycled concrete matrix to tensile loading. Similarly, Kilmartin-Lynch et al. [31] reported an approximately 12% increase in the tensile strength of normal aggregate concrete, confirming the positive effect of DMFM fiber on concrete strength. Samples with BF (0.25% and 0.5%) in hybrid mixes exhibited a higher increase in f'_{ST}. M4, M5, and M6 prepared with 0%, 0.1%, and 0.2% DMFM fiber and 0.25% BF exhibited f'_{ST} of 3.5 MPa, 3.7 MPa, and 3.8 MPa, representing increases of 11.2%, 16.5%, and 20.2%, respectively. Similarly, M7, M8, and M9 containing 0%, 0.1%, and 0.2% DMFM fiber and 0.5% BF exhibited f'_{ST} of 3.9 MPa, 4.1 MPa, and 3.9 MPa, representing increases of 22.9%, 26.1%, and 23.3%, respectively. The f'_{ST} for M9 indicated a slightly smaller increase, consistent with the compressive strength result, and higher than that of the reference sample. The increased performance of hybrid fiber-reinforced samples is related to improved microstructure quality with addition of DMFM fiber and BF. The SEM micrographs in Fig. 14 indicate uniform DMFM fiber and BF distribution, excellent interaction with the

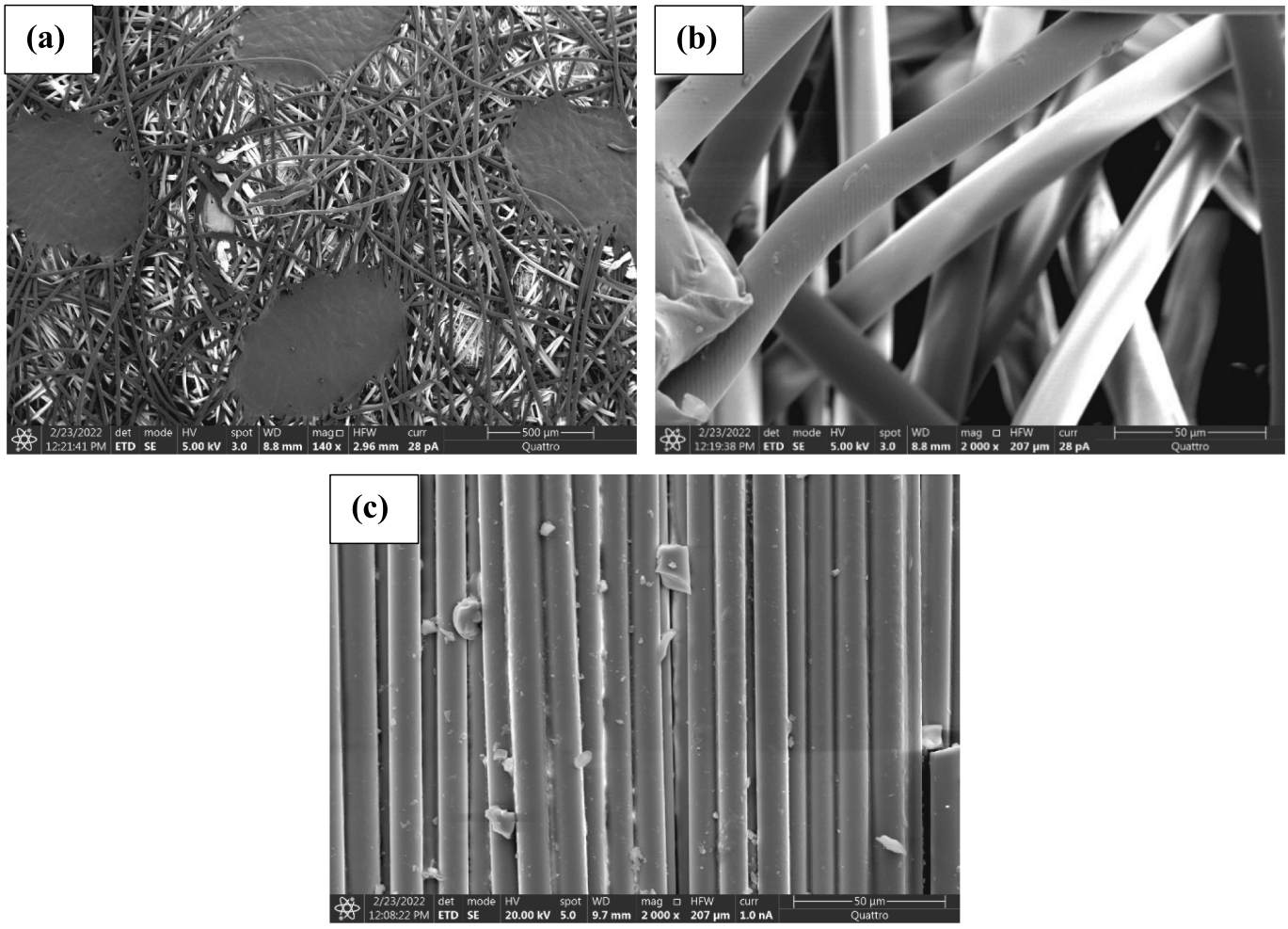

Fig. 9. (a) SEM image of DMFM fiber showing surface morphology of fibers and melting junction details; (b) SEM micrograph of inner layer of DMFM fiber showing shape and structure; (c) SEM micrograph of BF showing surface texture and shape.

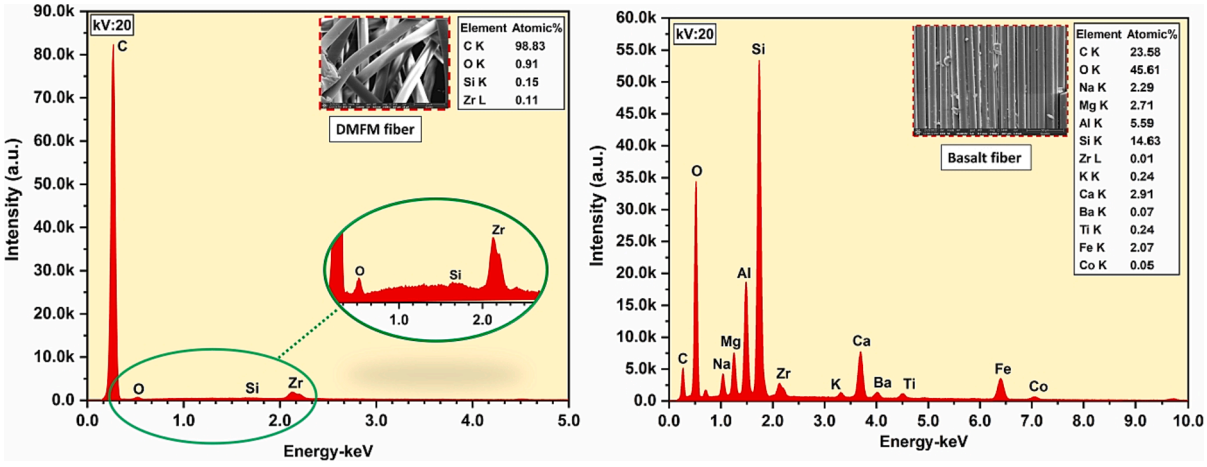

Fig. 10. SEM-EDAX spectra and elemental composition of DMFM fiber and basalt fiber.

adjacent cement mortar, and crack-arresting capabilities in the concrete matrix. DMFM fiber and BF are embedded in the cement mortar and their surfaces are covered by dense hydrated cement, confirming that they are highly compatible with the recycled concrete matrix.

4.4. Flexural strength

The results of flexural strength (f'_{FS}) tests of concrete prismatic beams are summarized in Fig. 15. The M0 and M1 samples (containing no fibers) exhibited an f'_{FS} of 3.31 MPa and 3.53 MPa, respectively. The slight increase in the f'_{FS} of M1 (6.6%) implies that the addition of FA and GGBFS in the FRAC improves concrete matrix quality, resulting in

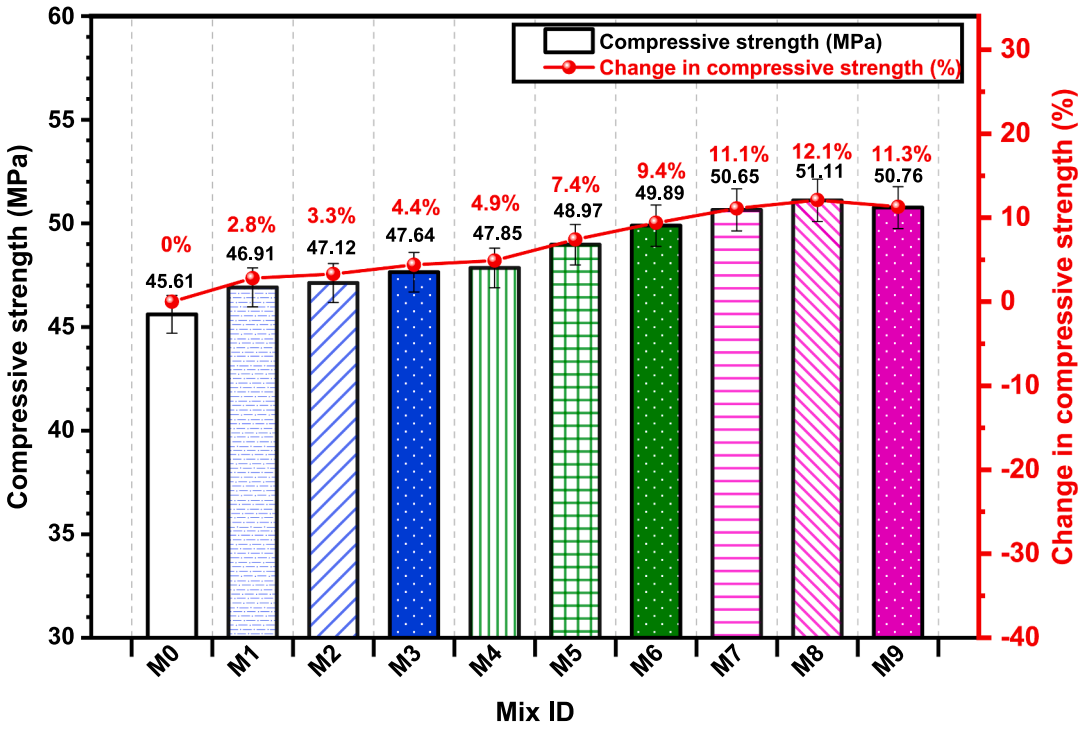

Fig. 11. Compressive strength (*f*'cs) of the reference sample and hybrid fiber-reinforced recycled concrete. The bar chart shows the compressive strength (MPa) of concrete samples (left axis); the line graph shows the change in compressive strength (%) of concrete samples (right axis).

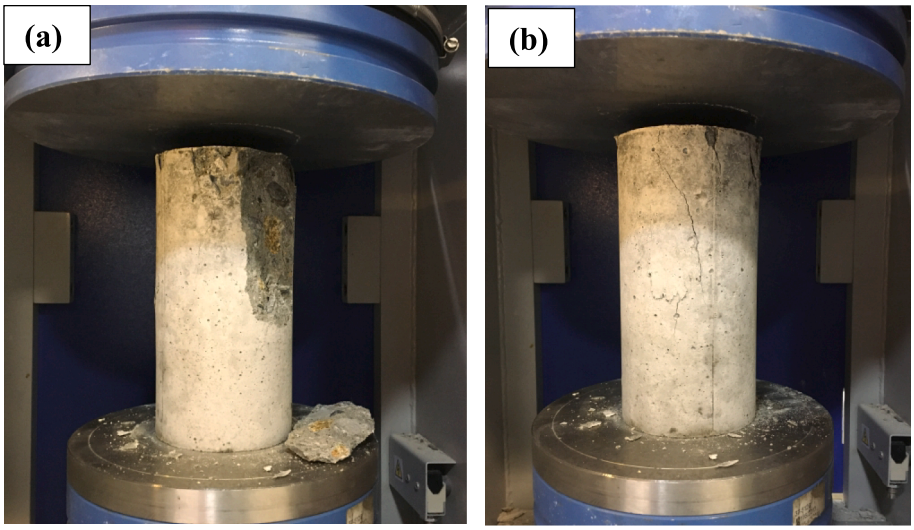

Fig. 12. Failure mode of reference sample (M0) and hybrid fiber-reinforced concrete sample (M8) after reaching ultimate compression capacity.

increased flexural strength. M2-M8 mixes exhibited a steady increase in f'_{FS} with increasing volume fractions of DMFM fiber and BF, similar to their compressive strength and tensile strength results. The f'_{FS} of M2 and M3 containing 0.1% and 0.2% DMFM fiber increased to 3.77 MPa and 3.95 MPa, respectively. The f'_{FS} increased further with combined use of DMFM fiber and BF. M4, M5, and M6 containing 0%, 0.1%, and 0.2% DMFM fiber and 0.25% BF exhibited f'_{FS} of 4.15 MPa, 4.45 MPa, and 4.89 MPa, respectively. Similarly, M7, M8, and M9 prepared with 0%, 0.1%, and 0.2% DMFM fiber and 0.5% BF exhibited f'_{FS} of 5.05 MPa, 5.28 MPa, and 5.24 MPa, respectively. The best performance was demonstrated by M8, with an increase in f'_{FS} of 59.5% in f'_{FS} compared to the control mix, consistent with the *f*'cs and f'_{ST} results. For M9, a slight decrease in f'_{FS} was observed; this trend was also observed for *f*'cs and f'_{ST}, and may be due to the negative effect of high doses of DMFM fiber and BF, as reported in previous studies [58,59]. Overall, the graph indicates improvements in the f'_{FS} of FRAC with combined use of DMFM fiber and BF, confirming the effectiveness of these fibers in strengthening the concrete microstructure and enabling resistance to high tensile stresses and cracking.

4.5. Density and UPV

Density and UPV are essential parameters that help assess the homogeneity and quality of a concrete mix. Fig. 16 shows the density and UPV test results for the reference and hybrid fiber-modified samples after curing. The reference sample had a density of 2393.25 kg/m^3 and UPV of 4477.27 m/s, which were lower than for all other fiber-modified samples, mainly due to the weak recycled concrete aggregate with

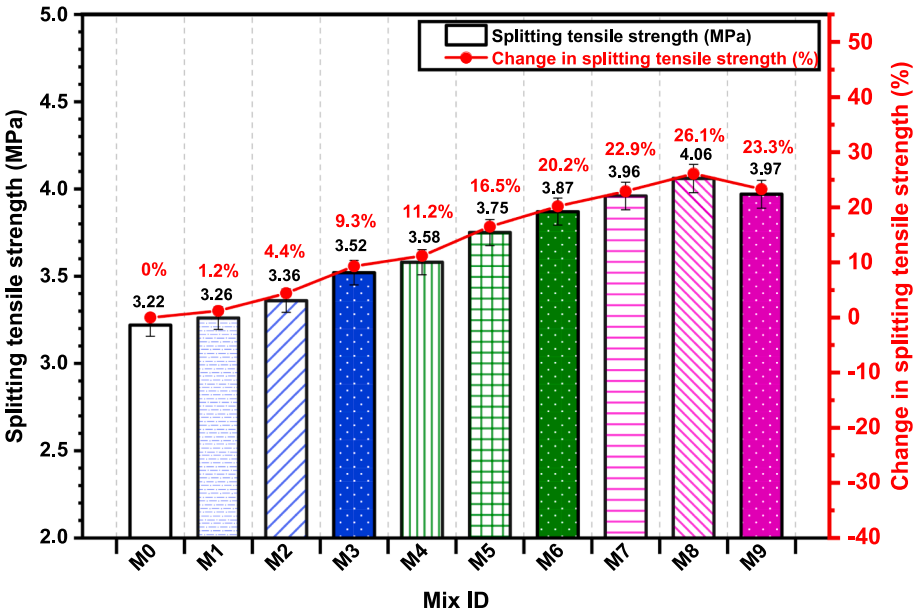

Fig. 13. Splitting tensile strength (f'_{ST}) of reference sample and hybrid fiber-reinforced recycled concrete. The bar chart indicates the splitting tensile strength (MPa) of concrete samples (left axis); the line graph indicates the change in splitting tensile strength (%) of concrete samples (right axis).

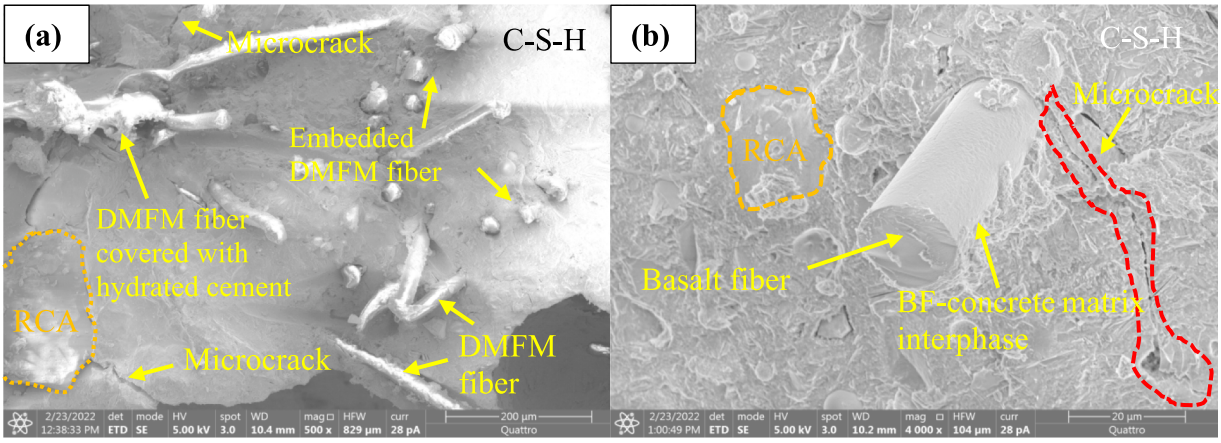

Fig. 14. SEM micrographs of hybrid fiber-reinforced recycled concrete showing the interaction of fiber material with host concrete matrix: (a) DMFM fiber; (b) BF.

unwanted voids and cavities that degrade concrete quality [43]. The density and UPV of DMFM fiber- and BF-reinforced samples M2-M9 ranged from 2406 kg/m^3–2433 kg/m^3 and 4502 m/s–4541 m/s, respectively. The microstructure compositions of FRAC samples were better than that of the reference sample, with fewer voids and pores, resulting in improved density and UPV. This confirms the usefulness of FA and GGBFS in counteracting microstructure defects that generally result from the inclusion of recycled aggregates in a concrete mix. The UPV of DMFM fiber- and BF-modified samples is greater than 4,500 m/s, which indicates a high-quality concrete mix that can be used for structural applications [60,61].

4.6. Water absorption

Water absorption of the reference and hybrid fiber-based samples is presented in Fig. 17. The water absorption of M0 was 2.22%, possibly attributed to the weak and porous microstructure of the concrete with inclusion of RCA [43,62]. M1 exhibited a slightly lower water absorption (1.68%), suggesting that addition of mineral admixtures FA and GGBFS was beneficial in reducing the number of voids and pores in the recycled concrete matrix. According to published literature, the use of FA and GGBFS results in production of calcium silicate hydrate (C-S-H) and calcium alumino-silicate hydrate (C-A-S-H) gels that improve the overall density and decrease the void space and permeability of the concrete [63,64].

Fig. 17 indicates an increase in the water absorption of concrete with increasing doses of DMFM fiber and BF. The highest water absorption was observed in the case of M9 (3.61%), mainly due to the congested network of DMFM fiber (Fig. 9(a)), resulting in unwanted cavities and pores inside the concrete matrix and increasing water absorption. The SEM micrograph of the M9 shown in Fig. 18 indicates several large voids and micropores in the vicinity of DMFM fiber and cement mortar that increase water absorption of the concrete [65]. Nevertheless, the water absorption of DMFM fiber- and BF-reinforced FRAC is still within the allowable water absorption limit for construction materials [66].

4.7. Synergy of DMFM fiber and BF

To further understand the synergy of DMFM fiber and BF in enhancing FRAC performance, the enhancement coefficients β_{CS}, β_{ST}, and β_{FS} were determined for different fiber combinations, as shown in Fig. 19, Fig. 20, and Fig. 21, respectively. These enhancement

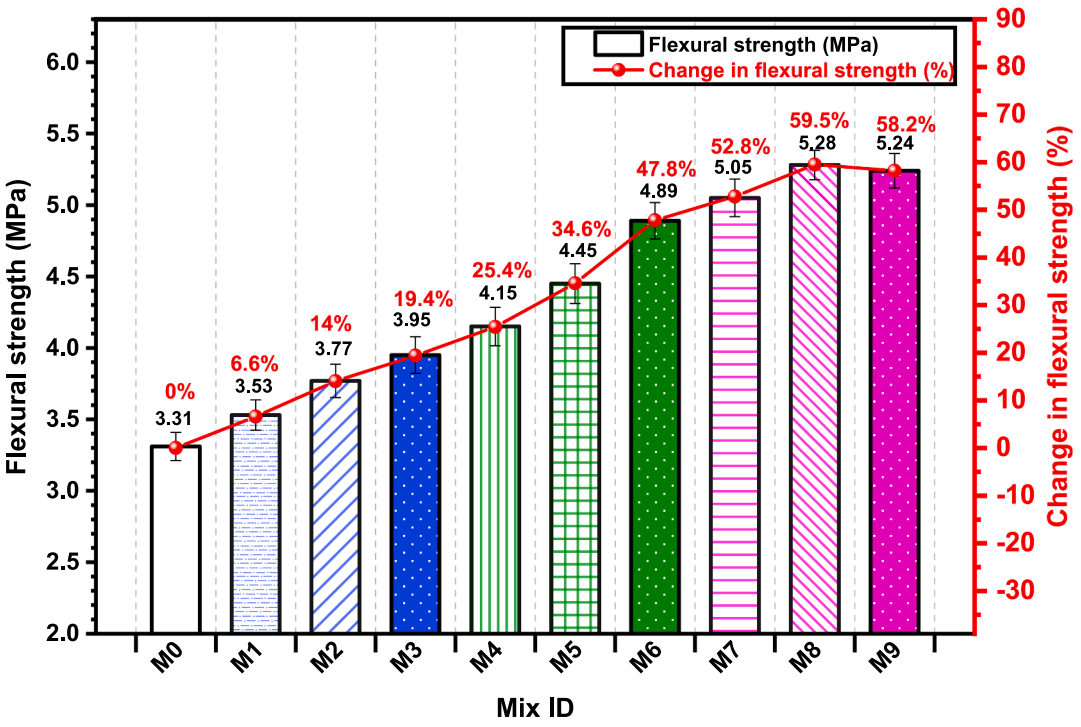

Fig. 15. Flexural strength (f'_{FS}) of reference sample and hybrid fiber-reinforced recycled concrete. The bar chart shows the flexural strength (MPa) of concrete samples (left axis); the line graph shows the change in flexural strength (%) of concrete samples (right axis).

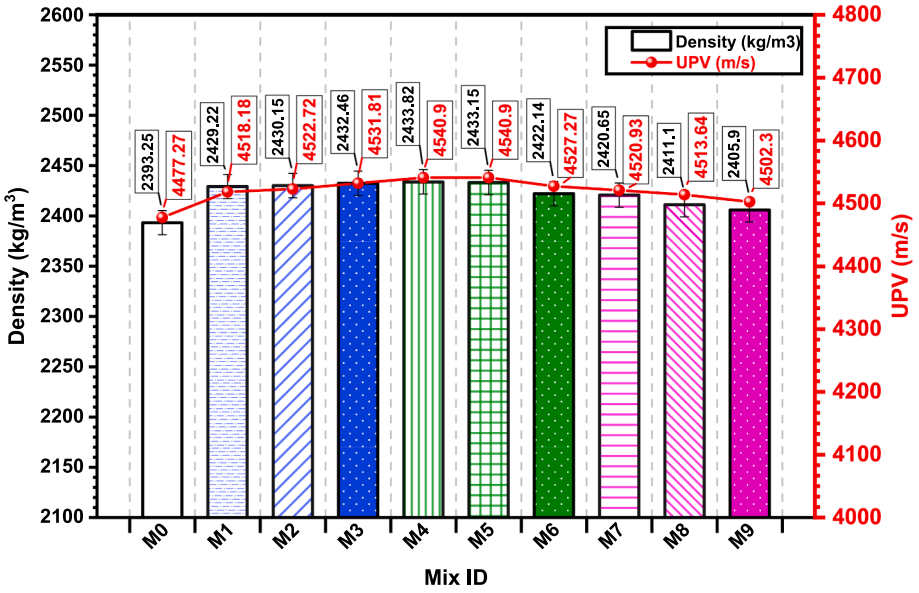

Fig. 16. Density and UPV of reference and hybrid fiber-reinforced FRAC. The bar chart shows the density (kg/m^3) of concrete samples (left axis); the line graph shows the UPV (m/s) of concrete samples (right axis).

coefficients indicate the ratio of the strength (f'_{CS}, f'_{ST}, and f'_{FS}) of a fiber-reinforced sample to the strength of the control sample (M0). Comparison of these enhancement coefficients helps in evaluating the synergic effect of DMFM fiber and BF in FRAC [67]. In Figs. 19-21, it is observed that all enhancement coefficients are greater than 1.0, implying that the hybrid addition of DMFM fiber and BF improved the mechanical performance of the FRAC. Furthermore, there is a steadily increasing trend in β_{CS}, β_{ST}, and β_{FS} with increase in the combined volume fractions of DMFM fiber and BF. The highest β_{CS} is 1.121; the highest β_{ST} is 1.261, and the highest β_{FS} is 1.595, all with a 0.1% volume fraction of DMFM fiber and 0.5% volume fraction of BF, indicating that the hybrid use of DMFM fiber and BF in FRAC produces a synergistic effect with better mechanical performance than with individual use of these fibers. Comparison of β_{CS}, β_{ST}, and β_{FS} with individual use of DMFM fiber and BF indicated that the latter is more effective in improving the mechanical performance of FRAC, mainly due to small diameter and high tensile strength; it improves the concrete microstructure via its crack-reinforcing and bridging abilities and increases the overall mechanical properties of FRAC.

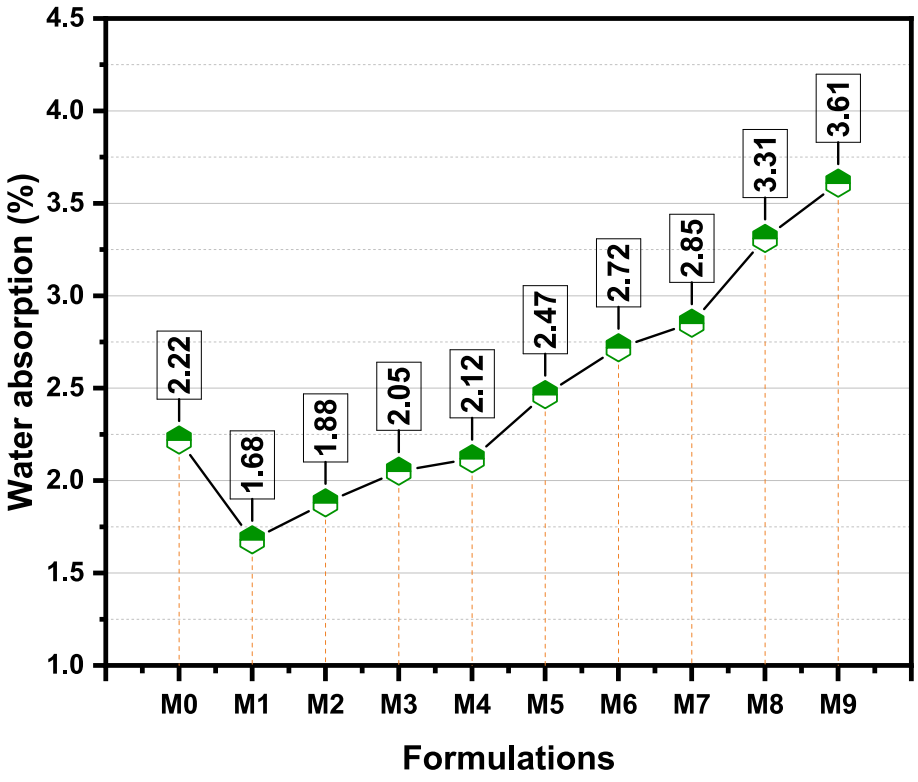

Fig. 17. Water absorption of reference and hybrid fiber-reinforced FRAC.

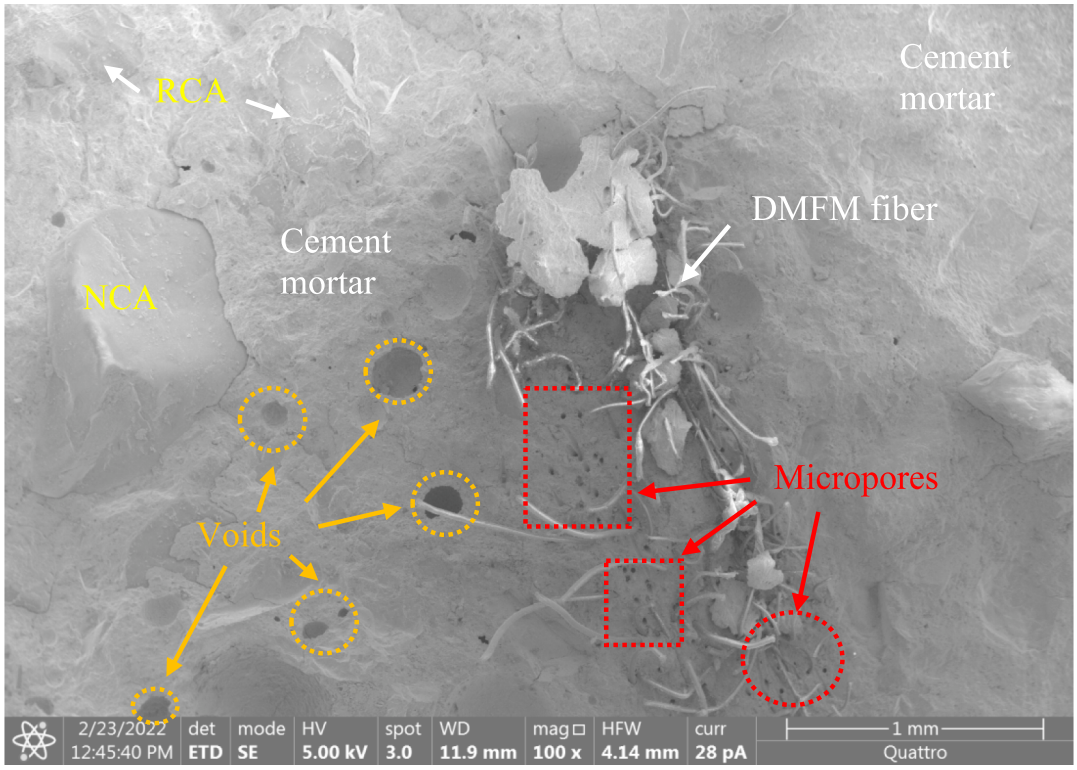

Fig. 18. SEM micrograph of M9 showing voids and micropores in vicinity of DMFM fiber and cement mortar interphase.

4.8. Microstructure investigation

The microstructures of the reference and hybrid fiber-modified concrete samples were observed with a Thermo Fisher Scientific Quattro S scanning electron microscope. The micrographs of the reference sample (M0) are shown in Fig. 22(a, b), and indicate a relatively weak concrete mix composition with poor bonding, especially in ITZs between cement mortar and NCA, and cement mortar and RCA. There

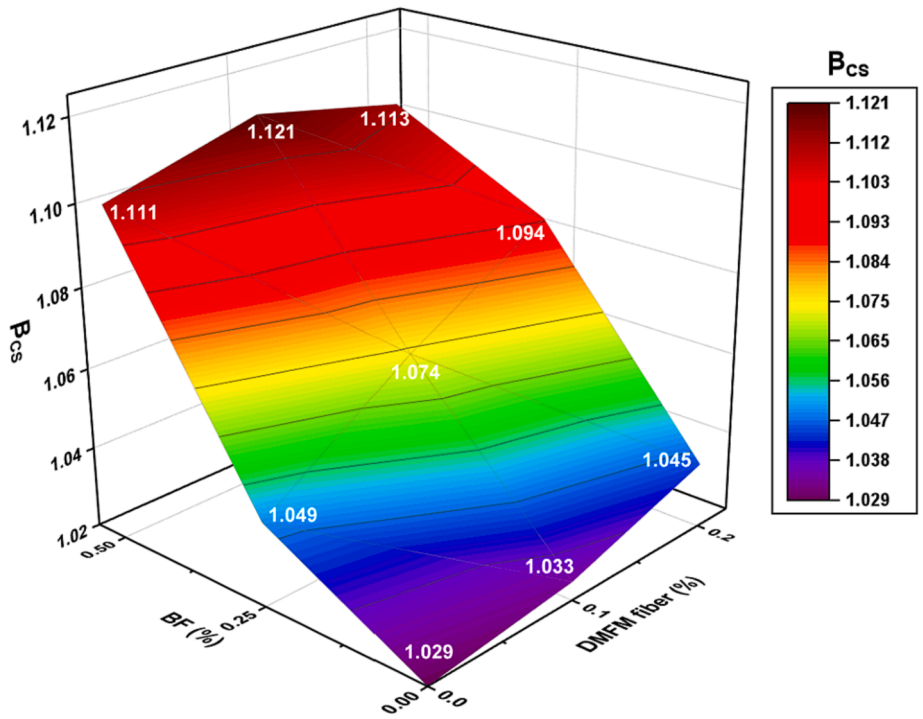

Fig. 19. Variation in β_{CS} of FRAC with different doses of DMFM fiber and BF.

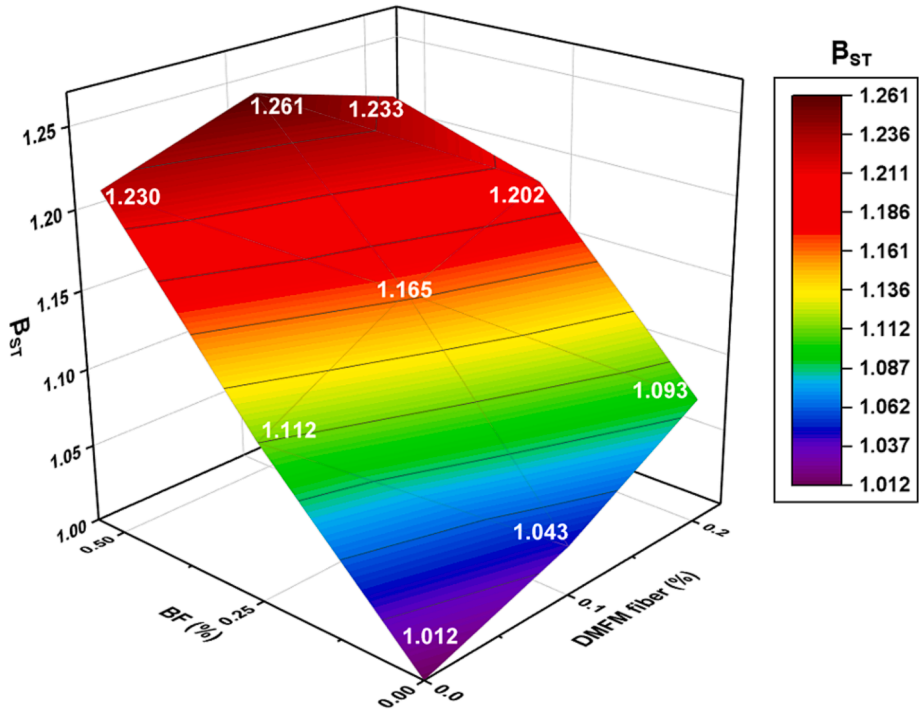

Fig. 20. Variation in β_{ST} of FRAC with different doses of DMFM fiber and BF.

are several microcracks within the cement mortar and in the ITZs, aggregate–cement interphases caused mainly by the weak RCA. These microstructural defects correlate with the low mechanical performance of M0 compared with the fiber-modified samples. The microstructure quality of M1 observed in Fig. 22(c, d) is improved consisting of dense cement mortar with fewer microcracks and voids than the reference mix. This may be attributed to combined use of FA and GGBFS, resulting in secondary C-S-H and C-A-S-H gels and enhancing the composition of the recycled concrete matrix [63,64]. The micrographs of DMFM fiber- and BF-reinforced FRAC shown in Fig. 22(e, f) indicate improved microstructure and excellent interaction between fibers and the host concrete matrix. The DMFM fibers are covered with cement mortar and BF are embedded in the concrete matrix, indicating good fiber-concrete matrix compatibility. In addition, the fiber materials, especially BF, were observed intercepting microcracks within the cement mortar, which is highly beneficial to FRAC in resisting tensile stress. Overall, it can be

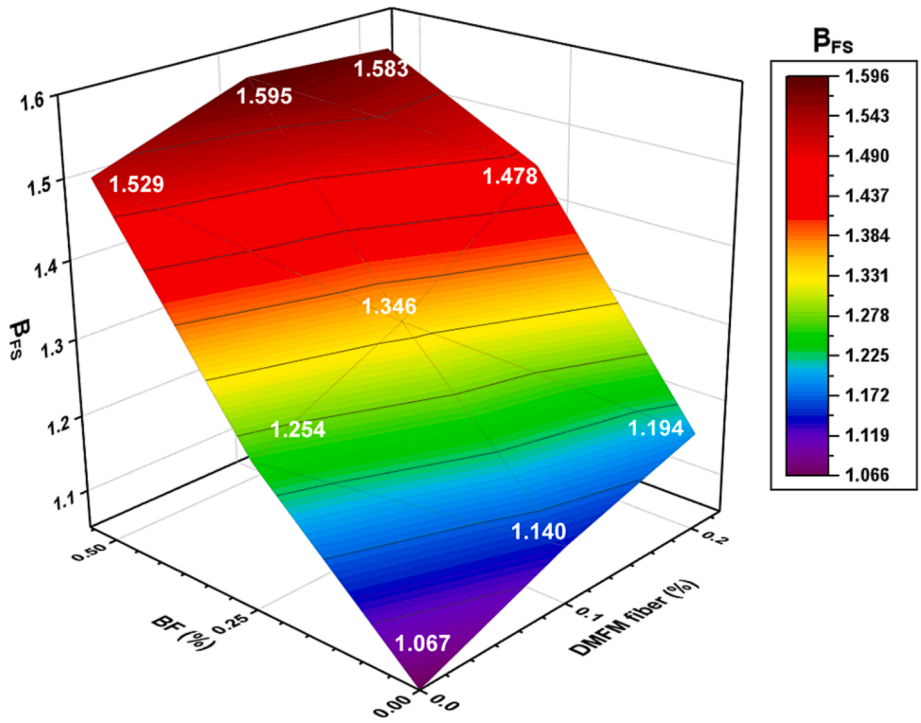

Fig. 21. Variation in β_{FS} of FRAC with different doses of DMFM fiber and BF.

inferred that the FRAC microstructure is greatly improved compared to the reference sample by the addition of mineral admixtures (FA and GGBFS) and hybrid fibers (DMFM fiber and BF). The improved microstructure correlates with the observed strength increases in FRAC.

5. Conclusions

In this study, we developed a new fiber-hybridization approach to recycle DMFMs as fiber materials for production of sustainable green recycled concrete. The technique is effective, eco-friendly, and highly beneficial in terms of improving the overall mechanical performance of FRAC and protecting the natural environment from rapidly increasing COVID-19 DMFM waste. From the findings of extensive laboratory tests, the following conclusions can be derived.

(i) The morphological investigation of DMFM fiber indicated a non-woven fabric surface morphology made of randomly distributed and closely spaced fibers joined through oval melting junction points. The inner layer of DMFM fiber had a smooth surface texture of thin PP fibers with an average diameter of approximately 20 μm. The micrograph of BFs showed a filament-type structure with a relatively smooth surface texture and no visible voids or pores.

(ii) The compressive strength test revealed that combined use of DMFM fiber and BF with the mineral admixtures (FA and GGBFS) increased the 28-day *f*'cs of FRAC. The 12% increase in the *f*'cs of FRAC can be attributed to the reinforcing action of hybrid fibers and the formation of secondary C-S-H and C-A-S-H gels due to the pozzolanic reaction of mineral admixtures.

(iii) From the splitting tensile test and flexural strength test, it was determined that the M8 sample (containing 0.1% DMFM fiber and 0.5% BF) produced the best results of all samples, with maximum increases of 26% in split tensile strength and 60% in flexural strength of FRAC.

(iv) The density and UPV of FRAC obtained with addition of mineral admixtures and hybrid fibers (0%, 0.1%, and 0.2% DMFM fiber and 0%, 0.25%, and 0.5% BF) ranged from 2406 kg/m^3–2433 kg/m^3 and 4502 m/s–4541 m/s, respectively, indicating high-quality concrete that can be used in structural concrete applications.

(v) The water absorption of FRAC slightly increased with increasing volume fractions of DMFM fiber and BF. A maximum water absorption of 3.61% was recorded for M9, which was prepared with 0.2% DMFM fiber and 0.5% BF. The water absorption was still well below the 10% permissible limit for construction materials.

(vi) The enhancement coefficients β_{CS}, β_{ST}, and β_{FS} of FRAC were greater than 1.0, indicating a positive synergy of DMFM fiber and BF. The optimum results were obtained with 0.1% volume fractions of DMFM fiber and 0.5% volume fractions of BF.

(vii) From the SEM micrographs of FRAC, it was concluded that the concrete microstructure composition, especially the ITZs between the RCA and cement mortar, was significantly improved with the addition of FA and GGBFS. Both DMFM fibers and BF indicated good compatibility with the host concrete matrix and effectively intercepted microcrack propagation contributing to better mechanical performance of FRAC.

(viii) Recycling DMFMs for use as reinforcing fiber in production of green sustainable FRAC is the most effective and eco-friendly path to resolving the global challenges caused by waste face masks. FRAC produced with the combined use of mineral admixtures and hybrid fibers (DMFM fiber and BF) exhibited an *f*'cs of greater than 50 MPa; thus, it can be used for building structures and other structural applications.

(ix) Overall, the experimental findings of this study suggest significant improvements in the mechanical performance of FRAC with combined use of DMFM fiber and BF. The effect of these fibers on post-cracking strength and long-term durability performance of FRAC will be explored in future research.

CRediT authorship contribution statement

Wisal Ahmed: Methodology, Formal analysis, Investigation, Data curation, Writing – original draft, Visualization. **C.W. Lim:** Conceptualization, Methodology, Project administration, Funding acquisition,

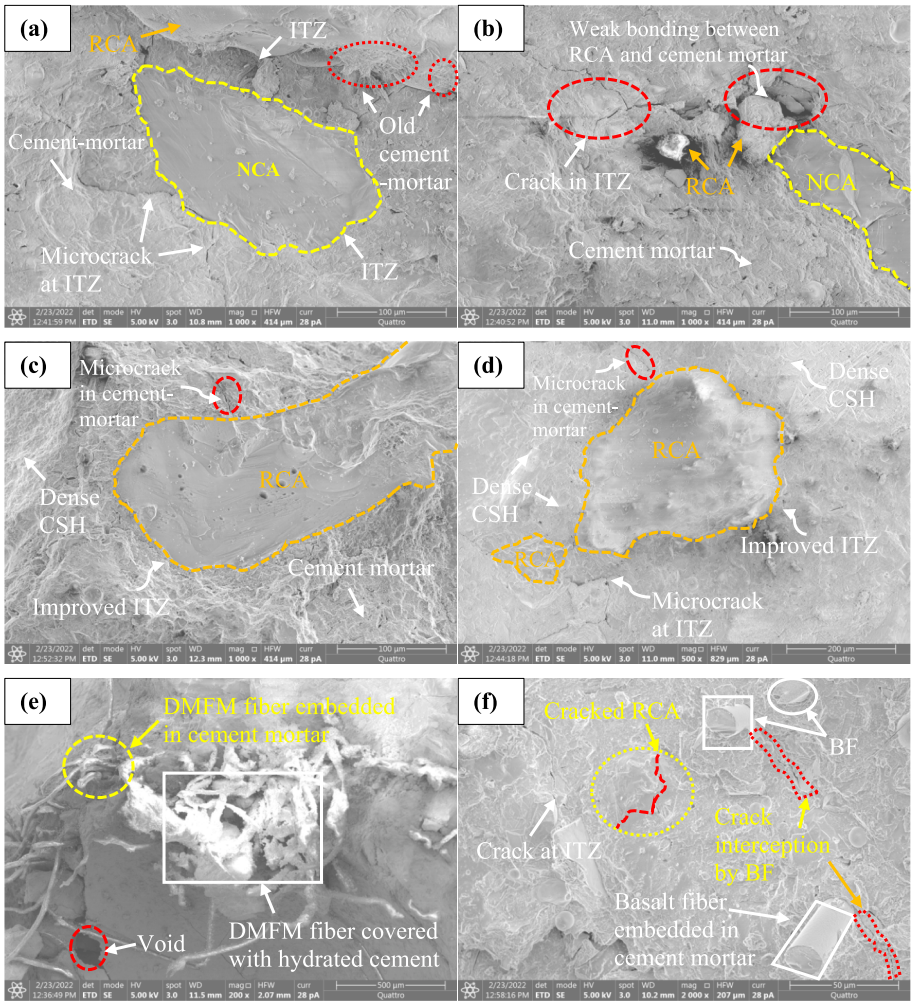

Fig. 22. SEM micrographs of reference and fiber-modified concrete samples demonstrating microstructure quality, ITZs, and fiber–matrix interaction: (a,b) Micrographs of M0 containing no fiber material; (c,d) Micrographs of M1 modified by addition of FA and GGBFS and containing no fiber material; (e,f) Micrographs of M8 modified by combined use of DMFM fiber and BF.

Resources, Supervision, Writing – review & editing.

Declaration of Competing Interest

The authors declare that they have no known competing financial interests or personal relationships that could have appeared to influence the work reported in this paper.

Acknowledgements

The work described in this paper was supported by City University of Hong Kong (Project No. ARG 9667219 and National Natural Science Foundation of China through a research grant awarded to City University of Hong Kong Shenzhen Research Institute (Project No. 12072165).

References

[1] World Health Organization (WHO), Tracking SARS-CoV-2 variants, (2022). https://www.who.int/en/activities/tracking-SARS-CoV-2-variants.
[2] O.P. Choudhary, M. Dhawan, Priyanka,, Omicron variant (B.1.1.529) of SARS-CoV-2: Threat assessment and plan of action, Int. J. Surg. 97 (2022), 106187, https://doi.org/10.1016/J.IJSU.2021.106187.
[3] C. Nzediegwu, S.X. Chang, Improper solid waste management increases potential for COVID-19 spread in developing countries, Resour. Conserv. Recycl. 161 (2020), 104947, https://doi.org/10.1016/J.RESCONREC.2020.104947.
[4] M. Saberian, J. Li, S. Kilmartin-Lynch, M. Boroujeni, Repurposing of COVID-19 single-use face masks for pavements base/subbase, Sci. Total Environ. 769 (2021), 145527, https://doi.org/10.1016/j.scitotenv.2021.145527.
[5] O.P. Priyanka, I. Choudhary, G. Singh, Patra, Aerosol transmission of SARS-CoV-2: The unresolved paradox, Travel Med. Infect. Dis. 37 (2020), https://doi.org/10.1016/J.TMAID.2020.101869.
[6] World Health Organization (WHO), Advice on the Use of Masks in the Community, During Home Care and in Healthcare Settings in the Context of the Novel Coronavirus (2019-nCoV) Outbreak., 1 (2020) 2. https://apps.who.int/iris/bitstream/handle/10665/330987/WHO-nCov-IPC_Masks-2020.1-eng.pdf?sequence=1&isAllowed=y.
[7] Y.T. Tesfaldet, N.T. Ndeh, J. Budnard, P. Treeson, Assessing face mask littering in urban environments and policy implications: The case of Bangkok, Sci. Total Environ. 806 (2022), 150952, https://doi.org/10.1016/J.SCITOTENV.2021.150952.
[8] G.E. De-la-Torre, M.R.J. Rakib, C.I. Pizarro-Ortega, D.C. Dioses-Salinas, Occurrence of personal protective equipment (PPE) associated with the COVID-19 pandemic along the coast of Lima, Peru, Sci. Total Environ. 774 (2021), 145774, https://doi.org/10.1016/j.scitotenv.2021.145774.
[9] J. Ammendolia, J. Saturno, A.L. Brooks, S. Jacobs, J.R. Jambeck, An emerging source of plastic pollution: Environmental presence of plastic personal protective equipment (PPE) debris related to COVID-19 in a metropolitan city, Environ. Pollut. 269 (2021), 116160, https://doi.org/10.1016/j.envpol.2020.116160.
[10] M. Thiel, D. de Veer, N.L. Espinoza-Fuenzalida, C. Espinoza, C. Gallardo, I. A. Hinojosa, T. Kiessling, J. Rojas, A. Sanchez, F. Sotomayor, N. Vasquez, R. Villablanca, COVID lessons from the global south – Face masks invading tourist beaches and recommendations for the outdoor seasons, Sci. Total Environ. 786 (2021), 147486, https://doi.org/10.1016/j.scitotenv.2021.147486.
[11] D.H.R. Spennemann, Covid face masks: Policy shift results in increased littering, Sustain. 13 (2021), https://doi.org/10.3390/su13179875.
[12] M. Ardusso, A.D. Forero-López, N.S. Buzzi, C.V. Spetter, M.D. Fernández-Severini, COVID-19 pandemic repercussions on plastic and antiviral polymeric textile causing pollution on beaches and coasts of South America, Sci. Total Environ. 763 (2021), https://doi.org/10.1016/j.scitotenv.2020.144365.

[13] J.C. Prata, A.L.P. Silva, T.R. Walker, A.C. Duarte, T. Rocha-Santos, COVID-19 Pandemic Repercussions on the Use and Management of Plastics, Environ. Sci. Technol. 54 (2020) 7760–7765, https://doi.org/10.1021/acs.est.0c02178.
[14] T.A. Aragaw, Surgical face masks as a potential source for microplastic pollution in the COVID-19 scenario, Mar. Pollut. Bull. 159 (2020), 111517, https://doi.org/10.1016/j.marpolbul.2020.111517.
[15] S. Akber Abbasi, A.B. Khalil, M. Arslan, Extensive use of face masks during COVID-19 pandemic: (micro-)plastic pollution and potential health concerns in the Arabian Peninsula, Saudi, J. Biol. Sci. 27 (2020) 3181–3186, https://doi.org/10.1016/j.sjbs.2020.09.054.
[16] E. Okuku, L. Kiteresi, G. Owato, K. Otieno, C. Mwalugha, M. Mbuche, B. Gwada, A. Nelson, P. Chepkemboi, Q. Achieng, V. Wanjeri, J. Ndwiga, L. Mulupi, J. Omire, The impacts of COVID-19 pandemic on marine litter pollution along the Kenyan Coast: A synthesis after 100 days following the first reported case in Kenya, Mar. Pollut. Bull. 162 (2021), 111840, https://doi.org/10.1016/j.marpolbul.2020.111840.
[17] R. Dhawan, B.M.S. Bisht, R. Kumar, S. Kumari, S.K. Dhawan, Recycling of plastic waste into tiles with reduced flammability and improved tensile strength, Process Saf. Environ. Prot. 124 (2019) 299–307, https://doi.org/10.1016/j.psep.2019.02.018.
[18] M. Boroujeni, M. Saberian, J. Li, Environmental impacts of COVID-19 on Victoria, Australia, witnessed two waves of Coronavirus, Environ. Sci. Pollut. Res. 28 (2021) 14182–14191, https://doi.org/10.1007/s11356-021-12556-y.
[19] T.P. Bondaroff, S. Cooke, Masks on the Beach: The impact of COVID-19, OCEANSASIA. (2020) 79. https://scholar.google.com/scholar_lookup?title=Masks on the beach%3A the impact of COVID-19 on marine plastic pollution&publication_year=2020&author=T.P. Bondaroff&author=S. Cooke.
[20] K.R. Vanapalli, H.B. Sharma, V.P. Ranjan, B. Samal, J. Bhattacharya, B.K. Dubey, S. Goel, Challenges and strategies for effective plastic waste management during and post COVID-19 pandemic, Sci. Total Environ. 750 (2021), 141514, https://doi.org/10.1016/j.scitotenv.2020.141514.
[21] K. Selvaranjan, S. Navaratnam, P. Rajeev, N. Ravintherakumaran, Environmental challenges induced by extensive use of face masks during COVID-19: A review and potential solutions, Environ. Challenges. 3 (2021), 100039, https://doi.org/10.1016/j.envc.2021.100039.
[22] W. Ahmed, C.W. Lim, Production of Sustainable and Structural Fiber Reinforced Recycled Aggregate Concrete with Improved Fracture Properties : A Review, J. Clean. Prod. 279 (2020) 1–42, https://doi.org/10.1016/j.jclepro.2020.123832.
[23] M. Idrees, A. Akbar, A.M. Mohamed, D. Fathi, F. Saeed, Recycling of waste facial masks as a construction material, a step towards sustainability, Materials (Basel) 15 (2022) 1–13, https://doi.org/10.3390/ma15051810.
[24] L. Wang, T. He, Y. Zhou, S. Tang, J. Tan, Z. Liu, J. Su, The influence of fiber type and length on the cracking resistance, durability and pore structure of face slab concrete, Constr. Build. Mater. 282 (2021), 122706, https://doi.org/10.1016/j.conbuildmat.2021.122706.
[25] H. Alabduljabbar, H. Mohammadhosseini, M.M. Tahir, R. Alyousef, Green and sustainable concrete production using carpet fibers waste and palm oil fuel ash, Mater. Today Proc. 39 (2021) 929–934, https://doi.org/10.1016/J.MATPR.2020.04.047.
[26] F. Alrshoudi, H. Mohammadhosseini, M.M. Tahir, R. Alyousef, H. Alghamdi, Y.R. Alharbi, A. Alsaif, Sustainable Use of Waste Polypropylene Fibers and Palm Oil Fuel Ash in the Production of Novel Prepacked Aggregate Fiber-Reinforced Concrete, Sustain. 2020, Vol. 12, Page 4871. 12 (2020) 4871. 10.3390/SU12124871.
[27] H. Mohammadhosseini, R. Alyousef, N.H. Abdul Shukor Lim, M.M. Tahir, H. Alabduljabbar, A.M. Mohamed, Creep and drying shrinkage performance of concrete composite comprising waste polypropylene carpet fibres and palm oil fuel ash, J. Build. Eng. 30 (2020) 101250. 10.1016/j.jobe.2020.101250.
[28] H. Mohammadhosseini, J.M. Yatim, A.R.M. Sam, A.S.M.A. Awal, Durability performance of green concrete composites containing waste carpet fibers and palm oil fuel ash, J. Clean. Prod. 144 (2017) 448–458, https://doi.org/10.1016/J.JCLEPRO.2016.12.151.
[29] W. Ahmed, C.W. Lim, A. Akbar, Influence of Elevated Temperatures on the Mechanical Performance of Sustainable-Fiber-Reinforced Recycled Aggregate Concrete: A Review, Build. 2022, Vol. 12, Page 487. 12 (2022) 487. 10.3390/BUILDINGS12040487.
[30] M. Koniorczyk, D. Bednarska, A. Masek, S. Cichosz, Performance of concrete containing recycled masks used for personal protection during coronavirus pandemic, Constr. Build. Mater. 324 (2022), 126712, https://doi.org/10.1016/j.conbuildmat.2022.126712.
[31] S. Kilmartin-Lynch, M. Saberian, J. Li, R. Roychand, G. Zhang, Preliminary evaluation of the feasibility of using polypropylene fibres from COVID-19 single-use face masks to improve the mechanical properties of concrete, J. Clean. Prod. 296 (2021), 126460, https://doi.org/10.1016/j.jclepro.2021.126460.
[32] Worldometer, World Population, (2022). https://www.worldometers.info/world-population/#region (accessed March 10, 2022).
[33] N.U. Benson, D.E. Bassey, T. Palanisami, COVID pollution: impact of COVID-19 pandemic on global plastic waste footprint, Heliyon 7 (2021) e06343.
[34] P.G. Ryan, C.J. Moore, J.A. Van Franeker, C.L. Moloney, Monitoring the abundance of plastic debris in the marine environment, Philos. Trans. R. Soc. B Biol. Sci. 364 (2009) 1999–2012, https://doi.org/10.1098/rstb.2008.0207.
[35] Y.T. Tesfaldet, N.T. Ndeh, Assessing face masks in the environment by means of the DPSIR framework, Sci. Total Environ. 814 (2022), 152859, https://doi.org/10.1016/j.scitotenv.2021.152859.
[36] K.O. Dowd, K.M. Nair, P. Forouzandeh, S. Mathew, J. Grant, R. Moran, J. Bartlett, J. Bird, S.C. Pillai, Face masks and respirators in the fight against the COVID-19 pandemic A review of current materials, advances and future perspectives, Materials (Basel). 13 (2020), https://doi.org/10.3390/ma13153363.
[37] H. Jamshaid, R. Mishra, A green material from rock: basalt fiber – a review, J. Text. Inst. 107 (2016) 923–937, https://doi.org/10.1080/00405000.2015.1071940.
[38] ASTM C150/C150M-20 Standard Specification for Portland Cement, (2020). https://www.astm.org/Standards/C150.htm.
[39] A. Gholampour, J. Zheng, T. Ozbakkaloglu, Development of waste-based concretes containing foundry sand, recycled fine aggregate, ground granulated blast furnace slag and fly ash, Constr. Build. Mater. 267 (2021), 121004, https://doi.org/10.1016/j.conbuildmat.2020.121004.
[40] ASTM C33/C33M, Standard Specification for Concrete Aggregates, (2016) 1–11. 10.1520/C0033.
[41] ASTM C494/494M, Standard Specification for Chemical Admixtures for Concrete, (2019). https://www.astm.org/Standards/C494.htm.
[42] G.M. Sadiqul Islam, S. Das Gupta, Evaluating plastic shrinkage and permeability of polypropylene fiber reinforced concrete, Int. J. Sustain Built Environ. 5 (2016) 345–354, https://doi.org/10.1016/j.ijsbe.2016.05.007.
[43] W. Ahmed, C.W. Lim, Coupling effect assessment of vacuum based pozzolana slurry encrusted recycled aggregate and basalt fiber on mechanical performance of fiber reinforced concrete, Constr. Build. Mater. 300 (2021), 124032, https://doi.org/10.1016/j.conbuildmat.2021.124032.
[44] A.I. Al-Hadithi, A.T. Noaman, W.K. Mosleh, Mechanical properties and impact behavior of PET fiber reinforced self-compacting concrete (SCC), Compos. Struct. 224 (2019), 111021, https://doi.org/10.1016/j.compstruct.2019.111021.
[45] ASTM C39/C39M, Standard Test Method for Compressive Strength of Cylindrical Concrete Specimens, (2020). https://www.astm.org/Standards/C39.
[46] ASTM C496/C496M, Standard Test Method for Splitting Tensile Strength of Cylindrical Concrete Specimens, (2017). https://www.astm.org/Standards/C496.
[47] ASTM C78/C78M, Standard Test Method for Flexural Strength of Concrete (Using Simple Beam with Third-Point Loading), (2018). https://www.astm.org/Standards/C78.
[48] ASTM C597, Standard Test Method for Pulse Velocity Through Concrete, (2016). https://www.astm.org/Standards/C597.htm.
[49] ASTM 642-06, Standard test method for density, absorption, and voids in hardened concrete, (2013). https://scholar.google.com/scholar_lookup?title=Standard Test Method for Density%2C Absorption%2C and Voids in Hardened Concrete&publication_year=2013&author=ASTM C 642–13.
[50] D. Battegazzore, F. Cravero, A. Frache, Is it possible to mechanical recycle the materials of the disposable filtering masks? Polymers (Basel) 12 (2020) 1–18, https://doi.org/10.3390/polym12112726.
[51] Z. Liu, D. Yu, Y. Ge, L. Wang, J. Zhang, H. Li, F. Liu, Z. Zhai, Understanding the factors involved in determining the bioburdens of surgical masks, Ann. Transl. Med. 7 (2019) 754–754. 10.21037/ATM.2019.11.91.
[52] U.N. Trieu Nguyen, K.H. Do, B. Jang, K.-S. Kim, J.-H. Kim, S.-M. Lee, Always-on photocatalytic antibacterial facemask with mini UV-LED array, Mater. Today Sustain. 18 (2022), 100117, https://doi.org/10.1016/j.mtsust.2022.100117.
[53] A. Ivanič, G. Kravanja, W. Kidess, R. Rudolf, S. Lubej, The influences of moisture on the mechanical, morphological and thermogravimetric properties of mineral wool made from basalt glass fibers, Materials (Basel) 13 (2020), https://doi.org/10.3390/ma13102392.
[54] S. Banchhor, M. Murmu, S.V. Deo, Combined effect of fly-ash and GGBS on performance of alkali activated concrete, J. Build. Pathol. Rehabil. 7 (2022) 1–6, https://doi.org/10.1007/S41024-022-00170-5/FIGURES/7.
[55] A. Rafeet, R. Vinai, M. Soutsos, W. Sha, Guidelines for mix proportioning of fly ash/GGBS based alkali activated concretes, Constr. Build. Mater. 147 (2017) 130–142, https://doi.org/10.1016/J.CONBUILDMAT.2017.04.036.
[56] M. Khan, M. Cao, C. Xie, M. Ali, Effectiveness of hybrid steel-basalt fiber reinforced concrete under compression, Case Stud. Constr. Mater. 16 (2022) e00941.
[57] H. Mohammadhosseini, Jamaludin, M. Yatim, Evaluation of the Effective Mechanical Properties of Concrete Composites Using Industrial Waste Carpet Fiber, Ina. Lett. 2017 21. 2 (2017) 1–12. 10.1007/S41403-017-0016-X.
[58] S. Rawat, R. Narula, N. Upasani, G. Muthukumar, A Relook on Dosage of Basalt Chopped Fibres and Its Influence on Characteristics of Concrete, Lect. Notes Civ. Eng. 38 (2020) 239–248, https://doi.org/10.1007/978-981-13-7615-3_22.
[59] T. Ochi, S. Okubo, K. Fukui, Development of recycled PET fiber and its application as concrete-reinforcing fiber, Cem. Concr. Compos. 29 (2007) 448–455, https://doi.org/10.1016/j.cemconcomp.2007.02.002.
[60] S.P. Yap, U.J. Alengaram, M.Z. Jumaat, Enhancement of mechanical properties in polypropylene- and nylon-fibre reinforced oil palm shell concrete, Mater. Des. 49 (2013) 1034–1041, https://doi.org/10.1016/j.matdes.2013.02.070.
[61] J.M. Khatib, B.A. Herki, A. Elkordi, Characteristics of concrete containing EPS, Elsevier Ltd (2019), https://doi.org/10.1016/b978-0-08-102676-2.00007-4.
[62] M.S. De Juan, P.A. Gutierrez, Study on the influence of attached mortar content on the properties of recycled concrete aggregate, Constr. Build. Mater. 23 (2009) 872–877, https://doi.org/10.1016/j.conbuildmat.2008.04.012.
[63] J.L. Provis, R.J. Myers, C.E. White, V. Rose, J.S.J. Van Deventer, X-ray microtomography shows pore structure and tortuosity in alkali-activated binders, Cem. Concr. Res. 42 (2012) 855–864, https://doi.org/10.1016/j.cemconres.2012.03.004.
[64] W.M. Shaban, J. Yang, H. Su, Q.-F. Liu, D.C.W. Tsang, L. Wang, J. Xie, L. Li, Properties of recycled concrete aggregates strengthened by different types of pozzolan slurry, Constr. Build. Mater. 216 (2019) 632–647.

[65] S. Yang, X. Yue, X. Liu, Y. Tong, Properties of self-compacting lightweight concrete containing recycled plastic particles, Constr. Build. Mater. 84 (2015) 444–453, https://doi.org/10.1016/j.conbuildmat.2015.03.038.
[66] C.B. Cheah, M. Ramli, The implementation of wood waste ash as a partial cement replacement material in the production of structural grade concrete and mortar: An overview, Resour. Conserv. Recycl. 55 (2011) 669–685, https://doi.org/10.1016/j.resconrec.2011.02.002.
[67] B. Lei, W. Li, H. Liu, Z. Tang, V.W.Y. Tam, Synergistic effects of polypropylene and glass fiber on mechanical properties and durability of recycled aggregate concrete, Int. J. Concr. Struct. Mater. 14 (2020) 1–14, https://doi.org/10.1186/s40069-020-00411-2.